



NUMERICAL MODELING OF A TRANSIENT STATE EVAPORATOR USING OBJECT-ORIENTED PROGRAMMING

Tesis para obtener el grado académico de Magíster en Energía que presenta:

AUTOR:

Jian Eduardo CARDENAS CABEZAS

ASESORES:

PhD. Alexandre VAUDREY

MSc. Enrique Jose BARRANTES PEÑA

Lyon - Mayo, 2023

Informe de Similitud


Yo, Enrique José Barrantes Peña, docente de la Escuela de Posgrado de la Pontificia Universidad Católica del Perú, asesor de la tesis de Maestría, titulada: "Numerical Modeling of a Transient state Evaporator using object-oriented programming"

De Jian Eduardo Cardenas Cabezas, dejo constancia de lo siguiente:

- El mencionado documento tiene un índice de puntuación de similitud de **15%**. Así lo consigna el reporte de similitud emitido por el software *Turnitin* el 25/04/2023.
- He revisado con detalle dicho reporte y la Tesis o Trabajo de Suficiencia Profesional, y no se advierte indicios de plagio.
- Las citas a otros autores y sus respectivas referencias cumplen con las pautas académicas.

Lugar y fecha:

San Miguel, 27 de abril de 2023

Apellidos y nombres del asesor: <u>Barrantes Peña, Enrique José</u>	
DNI: 07913376	Firma 
ORCID: 0000-0002-9037-3358	

Abstract

This work presents the dynamic modeling of a refrigeration machine evaporator that uses CO_2 (R744) as refrigerant fluid, for the cooling down of a liquid water stream, as required for instance by buildings air handling units. The main goal of such a work is to accurately model the transient evolution of the evaporator outlet *superheat*, which is one of the main parameters to control, due to its importance in refrigeration systems. A high value of superheat temperature reduces the performance of the system, while a low or null value can generate the suction of liquid which damages the compressor.

The theory of *moving boundaries* [19] with grouped parameters has been used for so. This method allows a precise resolution with a low numerical weight. In this method, the evaporator is divided into only two regions: the two phase region and superheated steam region, in which the energy conservation and mass conservation equations are solved. By using only two control volumes, the number of equations to be solved is smaller, thus reducing the calculation time. The ultimate aim of this work is to serve as a mathematical model usable for the design of efficient refrigeration system *controllers*, which are one of the most practical ways to improve the performance of these machines.

The results of a numerical analysis and of a sensitivity analysis, regarding to the influence of the heat convection coefficient of the two phase region, are also presented. For this sensitivity analysis, the maximum and minimum values available in the literature, see reference [7], have been used. According to this study, the convective coefficient of CO_2 varies from 8000 to 12000 $W \cdot m^{-2} \cdot K^{-1}$.

From this sensitivity analysis, it is observed that, despite the previously mentioned uncertainty about the convective coefficient value, the latter is not influential on the rest of the calculations and on parameters such as internal pressure, length of the two-phase lengths or superheat value. This is due to the fact that the thermal resistance of the liquid hot fluid is much higher than the cold fluid in the phase change region, the global heat transfer coefficient is thus more influenced by the hot fluid thermal resistance.

A maximum error of 3 percent is finally estimated in the determination of the transient superheat temperature.

Acknowledgment

I would first like to thank my project advisor PhD. Alexandre VAUDREY of the Energy Department at ECAM Lyon. The door to Prof. VAUDREY office was always open whenever I ran into a trouble spot or had a question about my project. His unconditional support even in the most difficult moments of my life is something I can never forget.

I would also like to thank the Director of the Master of Energy at Pontifical Catholic University of Peru, Mg. Fernando Jimenez, the Director of the Energy Department at ECAM Lyon, PhD. Vincent CAILLÉ, and the Director of International Relations at ECAM Lyon, Caroline HAN-RAS for giving me the opportunity to continue my studies at the PUCP and the ECAM Lyon in the framework of a double degree. To the PhD. Luis Chirinos who throughout this time was always aware of me giving me advice on how to improve at all times.

Finally, I must express my very profound gratitude to my parents for providing me with unflinching support and continuous encouragement throughout my years of study. This accomplishment would not have been possible without them. Thank you.

Index

Abstract	i
Acknowledgment	ii
Index	iii
Index of figures	v
Table index	vi
I Introduction	2
1.1 Context	2
1.2 Importance of control strategies	3
1.3 Objective	4
II Dynamic modeling of the evaporator	5
2.1 Moving boundaries model	5
2.2 Conservation of mass in Two phase region	6
2.3 Conservation of mass in the super heated region	8
2.4 Energy balance in the two phase region	9
2.5 Energy balance in the super-heated region	11
2.6 Mass conservation for the external fluid	12
2.7 Energy conservation for the external fluid	12
2.8 Combination of equations	13
III Solution algorithm development	18
3.1 Incorporation of thermodynamic properties	18
3.2 Variable initialization	18
3.3 Solving of differential equation	19
IV Numerical treatment of the model	22
4.1 Experimental correlations	22
4.2 Determination of length ℓ and total length of the evaporator	23
4.2.1 Calculation example	24
V Model exploitation	29

VI Conclusion and perspectives	34
Bibliography	36
Annex	39

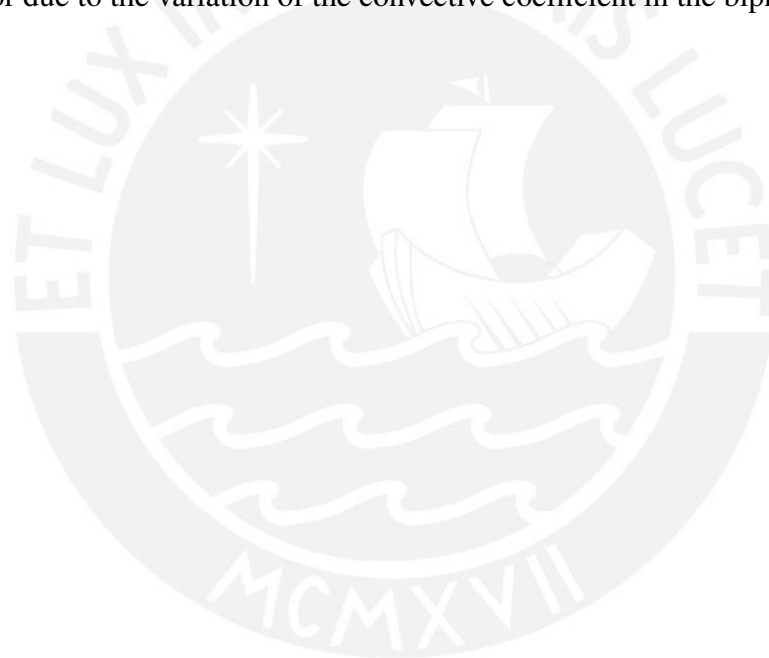


Index of figures

2.1	Diagram of the internal evaporator tube with a inner refrigerant and cold fluid flowing in counter-current to an outer hot fluid.	5
3.1	Flow Chart of the complete solving process.	19
3.2	Steady state flow chart.	20
4.1	Differential of heat transfer analysis.	24
4.2	Temperature variation in the evaporator	25
5.1	Mass flow vs time.	30
5.2	Mass velocity vs time.	30
5.3	Carbon dioxide pressure vs time.	31
5.4	Total heat flux vs time.	31
5.5	Outlet temperature vs time.	32
5.6	Carbon dioxide pressure vs time.	32
5.7	Total heat flux vs time.	33
5.8	Outlet temperature vs time.	33
0.1	Resistances in the two phase region	40

Table index

2.1	Array elements of differential equations	17
3.1	Array elements of matrix column in equation (3.2).	21
4.1	Input data for steady state calculation	22
5.1	Error due to the variation of the convective coefficient in the biphasic region	31



Nomenclature

Variable	Explanation	Units
A	Area	m^2
α	Convection heat transfer coefficient	$W/(m^2 \cdot K)$
γ	Void fraction	-
$\bar{\gamma}$	Mean void fraction	-
H, h	Enthalpy, Mass specific enthalpy	$J, J/kg$
L	Length	m
\dot{m}	mass flow rate	kg/s
P	Pressure	Pa
Pe	Perimeter	m
Q	Heat	J
Re	Reynold's number	-
ρ	density	kg/m^3
S	Slip ratio	-
T	Temperature	$^{\circ}C$
t	time	s
U, u	Internal energy, Mass specific internal energy	$J, J/kg$
UA	Lumped heat transfer coefficient	W/K
V	Volume	m^3
x	Quality	-
Subscript	Explanation	
c	Cold	
f	Liquid	
g	Vapor	
h	Hot	
in	In	
out	Out	

Chapter I

Introduction

1.1 Context

Refrigeration systems are widely used systems, they are found everywhere in the world [17]. At present, not only energy consumption is required to be able to carry out daily activities, but also a need has been created in which human beings require greater comfort to be able to carry out their activities. This is why refrigeration systems have progressively taken an fundamental place in the today's society. Refrigeration systems allow food to be preserved for a longer period of time, giving the opportunity to store the food and be transferred to any part of the world. Initially, ice or snow was used as natural sources for these purposes [10, 20], which gave rise to the unit of measurement used in this industry, which is the ton of refrigeration [14]. These systems are also widely used to provide cold water for air conditioning purposes in HVAC systems for commercial and industrial purposes [13].

On the other hand, the use of these systems, despite the great advantages and improvements in the quality of life that it implies, is detrimental to our environment. In this sense, various studies [21, 2, 19] have been carried out in order to reduce the amount of greenhouse effect emissions. In which refrigerant fluids such as CO_2 , which is friendly to the planet, have taken great relevance. In this sense, the present work uses CO_2 as a refrigerant fluid, in order to have a better understanding of the physical phenomena involved in its use.

Performance of refrigeration systems can be improved in two different situations. The first one is related to steady state operations, where a lot of effort have already been put into achieving the desired heat transfer with reasonable pressure drops. The second situation deals with the operation in the transient states, that is, the operation of the concerned machines along their starts, stops or load capacity variations periods. This thesis will focus on this last perspective because these machines operate under partial loads (outside their design point) and in a non-stationary state [8].

1.2 Importance of control strategies

Currently, refrigeration systems are constantly being improved in order to reach better energy performance. That is why control algorithms are constantly being developed to optimize the operation of these systems [9]. Controlling some specific parameter of the plant such as superheating in the evaporator, obtaining adequate superheating values that optimize the performance of the plant. However, the control engineers are often faced with the tedious challenge of developing simplified models of complex physical systems, and many times the development of these types of simplified models do not take into account the physical behavior of the studied system, thus giving a considerable error and a higher energy consumption [16].

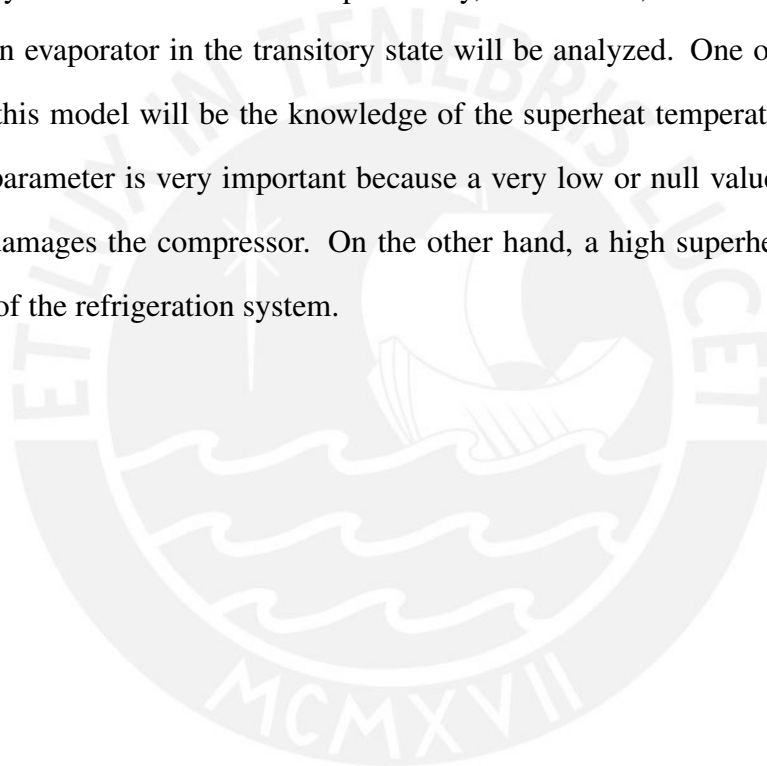
In the development of the simulation of a vapor compression refrigeration system, two main solution paradigms are obtained: models developed using the finite difference method and models that use moving boundaries [11]. In the finite difference paradigm, the mass, momentum and energy conservation equations are approximated with some finite difference technique to a finite number of elements in the heat exchanger [15]. Each element contains its own dynamic states. As the number of elements increases, the precision of the model also increases, the latter being its main interest [6]. However, the increase in the number of elements results in a dynamically complex model that can be computationally expensive and is not suitable for model-based control design [18].

The present work will focus on the dynamic modeling of the evaporator, a component

which is linked to the refrigeration machine, using for this the model of moving boundaries and grouped parameters. In this way, the proposed model will have fewer finite volumes to solve, making the model suitable for future development of a controller.

1.3 Objective

The objective of this thesis is to develop a mathematical model that is oriented to the control of refrigeration systems controllers. More specifically, in this work, the behavior of the refrigerant fluid within an evaporator in the transitory state will be analyzed. One of the most important outcomes of this model will be the knowledge of the superheat temperature at the evaporator outlet. This parameter is very important because a very low or null value can generate liquid suction that damages the compressor. On the other hand, a high superheat value reduces the performance of the refrigeration system.



Chapter II

Dynamic modeling of the evaporator

2.1 Moving boundaries model

In this chapter, the transient model of the the evaporator will be detailed. This component is very sensitive to transient variations. For the development of the dynamic model of the evaporator, the technique called moving boundaries with grouped parameters is used. The evaporator is considered as a tube within which there are two regions: one in which the fluid evaporates and is in a state of saturation, and the other in which the vapor is superheated (see Figure 2.1).

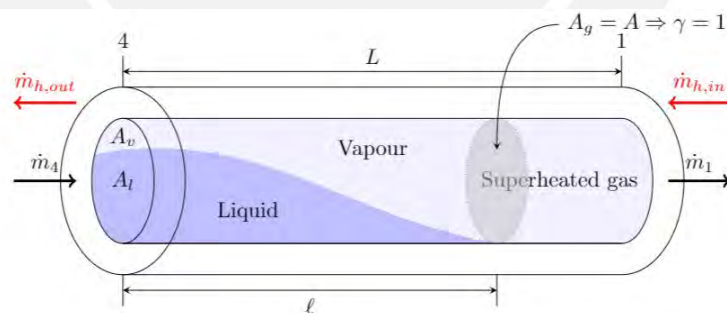


Figure 2.1: Diagram of the internal evaporator tube with a inner refrigerant and cold fluid flowing in counter-current to an outer hot fluid.

The hypotheses used in the development of the mathematical model are the following:

- The considered heat exchanger is modeled as a concentric type with a constant cross section for hot and cold flows.

- The pressure drop across the heat exchanger is neglected.
- Heat conduction within the refrigerant fluid is negligible.
- The kinetic energy and potential energy of fluids are neglected.
- The wall thermal resistance of the pipe is negligible in front of the hot and cold flows ones.

With these considerations, the mathematical model is developed to simulate the operation of an evaporator that has a two phase region and a region with superheating.

In order to develop the model, each region must be analyzed separately, that is, energy conservation and mass conservation must be carried out in each of these regions.

It is important to specify that until the moment of publication of the writing of this thesis, the modeling of the evaporators using the method of moving contours is carried out using the differential equations of the conservation of mass and energy, and then these equations are integrated throughout length of the evaporator using the Leibniz integration rule (for more information see [12, 3, 19]. In the present work the derivation of the equations was carried out using a physical approach.

2.2 Conservation of mass in Two phase region

The mass flow under concern, represented in Figure 2.1, is the one of a refrigerant fluid along an evaporator tube of constant cross sectional area A .

The total length of the tube is noted L , while ℓ corresponds to the length housing the fluid evaporation process. The remaining length $L - \ell$ corresponds to the superheat process of the fluid used to protect the downstream compressor against any harmful aspiration of liquid. With no compressibility effect inside the flow¹, the related instantaneous law of conservation of mass can be written as [4]:

$$\frac{dm}{dt}(t) = \dot{m}_4(t) - \dot{m}_\ell(t) \quad (2.1)$$

with \dot{m}_4 and \dot{m}_ℓ the inlet and outlet mass flow rates of the two phase region, respectively, and m the mass of fluid which is stored in this fraction of the tube (from 0 to ℓ) at time t . Considering

¹Since the Mach number is less than 0.3, it is stated that the flow is incompressible (See Appendix 3 in page 41).

the specific densities of the fluid as liquid and vapor, noted respectively ρ_l and ρ_v , this mass can also be expressed as [19]:

$$m = (\bar{\gamma} \cdot \rho_v + (1 - \bar{\gamma}) \cdot \rho_l) \cdot A \cdot \ell \quad (2.2)$$

$\bar{\gamma} \in [0; 1]$ is the average cross-sectional void fraction along the length ℓ , defined as :

$$\bar{\gamma} = \frac{1}{\ell} \cdot \int_0^\ell \gamma(z) \cdot dz \text{ with } \gamma = \frac{A_v}{A} = \frac{A_v}{A_v + A_l} \quad (2.3)$$

A_v and A_l are the parts of the cross-sectional area A which correspond to the presence of saturated vapor and liquid, respectively, and γ is the void fraction. Refrigerant fluid being pure within the flow, densities ρ_v and ρ_l are depending by definition on the evaporation temperature T_4 only. The mass m of fluid contained in the 0 to ℓ fraction of the tube at time t thus depends on four variables, namely $\bar{\gamma}$, ℓ , T_4 and T_1 . The time variation of m presented in the left part of equation (2.1) can thus be expressed as:

$$\frac{dm}{dt}(t) = \left(\frac{\partial m}{\partial \bar{\gamma}} \right)_{\ell,1,4} \cdot \frac{d\bar{\gamma}}{dt}(t) + \left(\frac{\partial m}{\partial \ell} \right)_{\bar{\gamma},1,4} \cdot \frac{d\ell}{dt}(t) + \left(\frac{\partial m}{\partial P} \right)_{\bar{\gamma},\ell,1} \cdot \frac{dP}{dt}(t) \quad (2.4)$$

with the partial derivative of mass m regarding to average void fraction $\bar{\gamma}$ obtained from (2.2):

$$\left(\frac{\partial m}{\partial \bar{\gamma}} \right)_{\ell,1,4} = (\rho_v - \rho_l) \cdot A \cdot \ell \quad (2.5)$$

In the very same way, the partial derivative of mass m regarding to length ℓ can be written as:

$$\left(\frac{\partial m}{\partial \ell} \right)_{\bar{\gamma},1,4} = (\bar{\gamma} \cdot \rho_v + (1 - \bar{\gamma}) \cdot \rho_l) \cdot A \quad (2.6)$$

The one regarding to pressure is:

$$\left(\frac{\partial m}{\partial P} \right)_{\bar{\gamma},\ell,4} = \left(\bar{\gamma} \cdot \frac{\partial \rho_v}{\partial P} + (1 - \bar{\gamma}) \cdot \frac{\partial \rho_l}{\partial P} \right) \cdot A \cdot \ell \quad (2.7)$$

It is worth noting that both of these expression are function of time t . The ordinary differential equation that ensure the conservation of mass inside the tube in Figure 2.1 can thus be expressed

as:

$$\begin{aligned} \frac{dm}{dt}(t) = & (\rho_v - \rho_l) \cdot A \cdot \ell \cdot \frac{d\bar{\gamma}}{dt} + (\bar{\gamma} \cdot \rho_v + (1 - \bar{\gamma}) \cdot \rho_l) \cdot A \cdot \frac{d\ell}{dt} \\ & + \left(\bar{\gamma} \cdot \frac{\partial \rho_v}{\partial P} + (1 - \bar{\gamma}) \cdot \frac{\partial \rho_l}{\partial P} \right) \cdot A \cdot \ell \cdot \frac{dP}{dt} \end{aligned} \quad (2.8)$$

This first order non-linear differential equation involves three different transient parameters: the average void fraction $\bar{\gamma}$, the length of the two-phase region ℓ and the refrigerant fluid pressure P .

2.3 Conservation of mass in the super heated region

In a similar way to what has been done in the two phase region, the mass of refrigerant inside the evaporator in the super heated region, ℓ to L , is given by (2.9):

$$m_{L-\ell} = \bar{\rho}_g \cdot A \cdot (L - \ell) \quad (2.9)$$

$\bar{\rho}_g$ is the average fluid density in this region, which can be expressed, for numerical computations purpose, as a function of pressure and average enthalpy ($\bar{\rho}_g = f(P, \bar{h}_g)$). The value of the average enthalpy \bar{h}_g can be approximated as the arithmetic mean of the enthalpy h_{out} at the outlet of the evaporator (L) and of the saturated vapor enthalpy h_v at $L - \ell$:

$$\bar{h}_g = \frac{h_v + h_{out}}{2}$$

Cross sectional area A being a constant, $m_{L-\ell}$ only depends on the $\bar{\rho}_g$ and ℓ values and the change in mass inside the ℓ to L fraction of the evaporator is given by the partial differentials of equation (2.9):

$$\frac{dm_{L-\ell}}{dt}(t) = \left(\frac{\partial m_{L-\ell}}{\partial \bar{\rho}_g} \right)_{\ell} \cdot \frac{d\bar{\rho}_g}{dt}(t) + \left(\frac{\partial m_{L-\ell}}{\partial \ell} \right)_{\bar{\rho}_g} \cdot \frac{d\ell}{dt}(t) \quad (2.10)$$

The variation of mass can also be expressed as [4]:

$$\frac{dm_{L-\ell}}{dt}(t) = \dot{m}_{\ell}(t) - \dot{m}_1(t) \quad (2.11)$$

In order to obtain the time variation of average density, the partial derivatives and the chain rule are used as a function of the independent variables, as shown in the equation (2.12):

$$\begin{aligned}\frac{d\bar{\rho}_g}{dt} &= \frac{\partial\bar{\rho}_g}{\partial P} \cdot \frac{dP}{dt} + \frac{\partial\bar{\rho}_g}{\partial\bar{h}_g} \cdot \frac{d\bar{h}_g}{dt} \\ &= \frac{\partial\bar{\rho}_g}{\partial P} \cdot \frac{dP}{dt} + \frac{\partial\bar{\rho}_g}{\partial\bar{h}_g} \left(\frac{1}{2} \cdot \frac{\partial h_v}{\partial P} \cdot \frac{dP}{dt} + \frac{1}{2} \cdot \frac{dh_{out}}{dt} \right)\end{aligned}\quad (2.12)$$

Replacing equation (2.12) in (2.10), we obtain:

$$\begin{aligned}\frac{dm_{L-\ell}}{dt} &= A \cdot (L - \ell) \cdot \left(\frac{\partial\bar{\rho}_g}{\partial P} \cdot \frac{dP}{dt} + \frac{\partial\bar{\rho}_g}{\partial\bar{h}_g} \left(\frac{1}{2} \cdot \frac{\partial h_v}{\partial P} \cdot \frac{dP}{dt} + \frac{1}{2} \cdot \frac{dh_{out}}{dt} \right) \right) - \bar{\rho}_g \cdot A \cdot \frac{d\ell}{dt} \\ &= A \cdot (L - \ell) \cdot \frac{\partial\bar{\rho}_g}{\partial P} \cdot \frac{dP}{dt} + A \cdot (L - \ell) \cdot \frac{1}{2} \frac{\partial\bar{\rho}_g}{\partial\bar{h}_g} \cdot \frac{dh_{out}}{dt} \\ &\quad + A \cdot (L - \ell) \cdot \frac{\partial\bar{\rho}_g}{\partial\bar{h}_g} \cdot \frac{1}{2} \cdot \frac{\partial h_v}{\partial P} \cdot \frac{dP}{dt} - \bar{\rho}_g \cdot A \cdot \frac{d\ell}{dt} \\ &= A \cdot (L - \ell) \cdot \left(\frac{\partial\bar{\rho}_g}{\partial P} + \frac{1}{2} \cdot \frac{\partial\bar{\rho}_g}{\partial\bar{h}_g} \cdot \frac{\partial h_v}{\partial P} \right) \cdot \frac{dP}{dt} + A \cdot (L - \ell) \cdot \frac{1}{2} \frac{\partial\bar{\rho}_g}{\partial\bar{h}_g} \cdot \frac{dh_{out}}{dt} - \bar{\rho}_g \cdot A \cdot \frac{d\ell}{dt}\end{aligned}\quad (2.13)$$

This differential equation involves three unknowns as well, pressure P and length ℓ as in equation (2.8), as well as the output enthalpy h_{out} .

2.4 Energy balance in the two phase region

The refrigerant fluid is supposed to be both lightweight and flowing through the evaporator at a relatively low speed. Its mass specific energy is then its sole enthalpy h . Because no friction effect is taken into account in the present model : (i) no specific equation is needed to represent the conservation of momentum, and (ii) no energy is dissipated because of the friction of the refrigerant fluid on the inner surface of the tube. The conservation of energy applied to the two phase region is then given by [4]:

$$\frac{dU_\ell}{dt} = \dot{Q}_\ell + \dot{m}_4 \cdot h_4 - \dot{m}(\ell) \cdot h(\ell)\quad (2.14)$$

U_ℓ is the internal energy of the matter contained in the two phase region. The heat rate \dot{Q} exchanged by the whole tube of length L across its external area $A_w = Pe \cdot L$ (Pe being the tube perimeter) will be divided into two parts : the first one \dot{Q}_ℓ related to the length ℓ and to the evaporation process at constant temperature T_4 , and the other one $\dot{Q}_{L-\ell}$ related to the length $L - \ell$ and to the superheat process at the average gas temperature \bar{T}_g . h_4 and h_1 are the mass specific enthalpies of the fluid at the evaporator inlet and outlet, respectively. Heat rates \dot{Q}_ℓ and $\dot{Q}_{L-\ell}$ can then be expressed as[5]:

$$\dot{Q}_\ell = \frac{\bar{T}_{h,\ell} - T_4}{R_\ell} \quad \dot{Q}_{L-\ell} = \frac{\bar{T}_{h,L-\ell} - \bar{T}_g}{R_{L-\ell}} \quad (2.15)$$

Where R_ℓ and $R_{L-\ell}$ represent the thermal resistances in the control volume of the two-phase region and the superheat region, respectively.

Introducing the enthalpy H_ℓ of the fluid in the two phase region, we can express the time derivative of internal energy of equation (2.14) as:

$$\begin{aligned} \frac{dU_\ell}{dt} &= \frac{d(H_\ell - P \cdot V)}{dt} = \frac{dH_\ell}{dt} - P \frac{dV}{dt} - V \frac{dP}{dt} = \frac{dH_\ell}{dt} - P \frac{d(A \cdot \ell)}{dt} - A \cdot \ell \cdot \frac{dP}{dt} \\ &= \frac{dH_\ell}{dt} - P \cdot A \cdot \frac{d\ell}{dt} - A \cdot \ell \cdot \frac{dP}{dt} \end{aligned} \quad (2.16)$$

With the time variation of enthalpy given by equation (2.17):

$$\begin{aligned} \frac{dH_\ell}{dt} &= \frac{\partial H_\ell}{\partial \bar{\gamma}} \cdot \frac{d\bar{\gamma}}{dt} + \frac{\partial H_\ell}{\partial P} \cdot \frac{dP}{dt} + \frac{\partial H_\ell}{\partial \ell} \cdot \frac{d\ell}{dt} \\ &= (\rho_v \cdot h_v - \rho_\ell \cdot h_\ell) \cdot A \cdot \ell \cdot \frac{d\bar{\gamma}}{dt} \\ &\quad + \left(\bar{\gamma} \left(\frac{\partial \rho_v}{\partial P} \cdot h_v + \frac{\partial h_v}{\partial P} \cdot \rho_v \right) \cdot \frac{dP}{dt} + (1 - \bar{\gamma}) \left(\frac{\partial \rho_\ell}{\partial P} \cdot h_\ell + \frac{\partial h_\ell}{\partial P} \cdot \rho_\ell \right) \cdot \frac{dP}{dt} \right) \cdot A \cdot \ell \\ &\quad + (\bar{\gamma} \cdot \rho_v \cdot h_v + (1 - \bar{\gamma}) \cdot \rho_\ell \cdot h_\ell) \cdot A \cdot \frac{d\ell}{dt} \end{aligned} \quad (2.17)$$

Replacing equation (2.17) in equation (2.16), we obtain:

$$\begin{aligned} \frac{dU_\ell}{dt} &= (\rho_v \cdot h_v - \rho_\ell \cdot h_\ell) \cdot A \cdot \ell \cdot \frac{d\bar{\gamma}}{dt} \\ &\quad + (\bar{\gamma} \cdot \rho_v \cdot h_v + (1 - \bar{\gamma}) \cdot \rho_\ell \cdot h_\ell - P) \cdot A \cdot \frac{d\ell}{dt} \\ &\quad + \left(\bar{\gamma} \left(\frac{\partial \rho_v}{\partial P} \cdot h_v + \frac{\partial h_v}{\partial P} \cdot \rho_v \right) + (1 - \bar{\gamma}) \left(\frac{\partial \rho_\ell}{\partial P} \cdot h_\ell + \frac{\partial h_\ell}{\partial P} \cdot \rho_\ell \right) - 1 \right) \cdot A \cdot \ell \cdot \frac{dP}{dt} \end{aligned} \quad (2.18)$$

This differential equation involves the same three parameters as the one (2.8) representing the conservation of mass.

2.5 Energy balance in the super-heated region

Analogously to the two-phase region, applying the first law of thermodynamics [4], we obtain:

$$\frac{dU_{L-\ell}}{dt} = \dot{Q}_{L-\ell} + \dot{m}(\ell) \cdot h_v - \dot{m} \cdot h_1 \quad (2.19)$$

The same variation can be expressed using the enthalpy $H_{L-\ell}$ of the refrigerant fluid in the same region:

$$\begin{aligned} \frac{dU_{L-\ell}}{dt} &= \frac{d(H_{L-\ell} - P \cdot V)}{dt} = \frac{dH_{L-\ell}}{dt} - P \cdot \frac{dV}{dt} - V \cdot \frac{dP}{dt} \\ &= \frac{dH_{L-\ell}}{dt} - P \cdot \frac{d(A \cdot (L - \ell))}{dt} - A \cdot (L - \ell) \cdot \frac{dP}{dt} \\ &= \frac{dH_{L-\ell}}{dt} + P \cdot A \cdot \frac{d\ell}{dt} - A \cdot (L - \ell) \cdot \frac{dP}{dt} \end{aligned} \quad (2.20)$$

With the enthalpy in the saturated vapor region given by:

$$H_{L-\ell} = \bar{\rho}_g \cdot \bar{h}_g \cdot A \cdot (L - \ell) \quad (2.21)$$

The variation of enthalpy with respect to time is given by the equation:

$$\begin{aligned} \frac{dH_{L-\ell}}{dt} &= \frac{d\bar{\rho}_g}{dt} \cdot \bar{h}_g \cdot A \cdot (L - \ell) + \bar{\rho}_g \cdot A \cdot (L - \ell) \frac{d\bar{h}_g}{dt} - \bar{\rho}_g \cdot \bar{h}_g \cdot A \frac{d\ell}{dt} \\ &= \left(\frac{\partial \bar{\rho}_g}{\partial P} \cdot \frac{dP}{dt} + \frac{\partial \bar{\rho}_g}{\partial \bar{h}_g} \left(\frac{1}{2} \cdot \frac{\partial h_v}{\partial P} \cdot \frac{dP}{dt} + \frac{1}{2} \cdot \frac{dh_{out}}{dt} \right) \right) \cdot \bar{h}_g \cdot A \cdot (L - \ell) \\ &\quad + \bar{\rho}_g \cdot A \cdot (L - \ell) \cdot \left(\frac{1}{2} \cdot \frac{\partial h_v}{\partial P} \frac{dP}{dt} + \frac{1}{2} \cdot \frac{dh_{out}}{dt} \right) - \bar{\rho}_g \cdot \bar{h}_g \cdot A \frac{d\ell}{dt} \end{aligned} \quad (2.22)$$

Replacing the value of the enthalpy variation (equation 2.22) in the equation 2.20 we have:

$$\begin{aligned} \frac{dU_{L-\ell}}{dt} &= \left(\frac{\partial \bar{\rho}_g}{\partial P} \cdot \bar{h}_g + \frac{\partial \bar{\rho}_g}{\partial \bar{h}_g} \cdot \frac{1}{2} \frac{\partial h_v}{\partial P} \cdot \bar{h}_g + \bar{\rho}_g \cdot \frac{1}{2} \cdot \frac{\partial h_v}{\partial P} - 1 \right) \cdot A \cdot (L - \ell) \cdot \frac{dP}{dt} \\ &\quad + \left(\frac{1}{2} \frac{\partial \bar{\rho}_g}{\partial \bar{h}_g} \cdot \bar{h}_g + \frac{1}{2} \bar{\rho}_g \right) \cdot A \cdot (L - \ell) \cdot \frac{dh_{out}}{dt} + (P - \bar{\rho}_g \cdot \bar{h}_g) \cdot A \cdot \frac{d\ell}{dt} \end{aligned} \quad (2.23)$$

As for the conservation of mass in the same region represented by equation (2.13), three transient parameters are involved, pressure P , enthalpy h_{out} and length ℓ .

2.6 Mass conservation for the external fluid

In the case of the external fluid (water in liquid state), in the present model, it is considered that it will not go through a phase change, so the amount of mass inside the heat exchanger is given by the following expression [4]:

$$m_{ex} = \bar{\rho}_{ex} \cdot A_e \cdot L \quad (2.24)$$

In a similar way to the previously developed cases, the law of mass conservation in this region is described by [4]:

$$\frac{dm_{ex}}{dt} = \dot{m}_{in,ex} - \dot{m}_{o,ex} \quad (2.25)$$

The variation of the external fluid mass in the heat exchanger with respect to time of the equation 2.25, is described by the equation 2.26, the which arises from applying the derivative with respect to time to the equation 2.24.

$$\frac{dm_{ex}}{dt} = A_e \cdot L \cdot \left(\frac{\partial \bar{\rho}_{ex}}{\partial P_{ex}} \cdot \frac{dP_{ex}}{dt} + \frac{1}{2} \cdot \frac{\partial \bar{\rho}_{ex}}{\partial h_{ex}} \cdot \frac{dh_{h,0}}{dt} \right) \quad (2.26)$$

2.7 Energy conservation for the external fluid

Applying the first law of thermodynamics for the external fluid [5], equation (2.27) is obtained.

$$\frac{dU_{ex}}{dt} = \underbrace{-\dot{Q}_\ell - \dot{Q}_{L-\ell}}_{=-\dot{Q}} + \dot{m}_{in,ex} \cdot h_{h,i} - \dot{m}_{o,ex} \cdot h_{h,o} \quad (2.27)$$

The variation of the internal energy with respect to time can also be described from the definition of absolute enthalpy and its subsequent derivation (equation 2.28), only that unlike the regions in the internal fluid, there is no variation in volume with respect to time.

$$\frac{dU_{ex}}{dt} = \frac{dH_{ex}}{dt} - V \cdot \frac{dP_{ex}}{dt} \quad (2.28)$$

Where the absolute enthalpy by definition is the, multiplication of the specific enthalpy by the total mass of the external fluid inside the heat exchanger, as shown in equation (2.29).

$$H_{ex} = m_{ex} \cdot \bar{h}_{ex} = \bar{\rho}_{ex} \cdot A_{ex} \cdot L \cdot \bar{h}_{ex} \quad (2.29)$$

From the equation (2.29), it is observed that the absolute enthalpy depends on 4 variables, of which only the density, $\bar{\rho}_{ex}$, and the specific enthalpy, \bar{h}_{ex} , vary with time. Therefore, deriving equation (2.29) with respect to time gives equation (2.30).

$$\begin{aligned} \frac{dH_{ex}}{dt} &= A_{ex} \cdot L \cdot \bar{h}_{ex} \cdot \frac{d\bar{\rho}_{ex}}{dt} + \bar{\rho}_{ex} \cdot A_{ex} \cdot L \cdot \frac{d\bar{h}_{ex}}{dt} \\ &= A_{ex} \cdot L \cdot \bar{h}_{ex} \cdot \left(\frac{\partial \bar{\rho}_{ex}}{\partial P_{ex}} \cdot \frac{dP_{ex}}{dt} + \frac{1}{2} \cdot \frac{\partial \bar{\rho}_{ex}}{\partial \bar{h}_{ex}} \cdot \frac{dh_{h,o}}{dt} \right) + \bar{\rho}_{ex} \cdot A_{ex} \cdot L \cdot \frac{1}{2} \cdot \frac{dh_{h,o}}{dt} \\ &= A_{ex} \cdot L \cdot \bar{h}_{ex} \cdot \frac{\partial \bar{\rho}_{ex}}{\partial P_{ex}} \cdot \frac{dP_{ex}}{dt} + \frac{1}{2} \cdot A_{ex} \cdot L \cdot \left(\bar{h}_{ex} \cdot \frac{\partial \bar{\rho}_{ex}}{\partial \bar{h}_{ex}} + \bar{\rho}_{ex} \right) \cdot \frac{dh_{h,o}}{dt} \end{aligned} \quad (2.30)$$

Replacing equation (2.30) in (2.28), we have:

$$\frac{dU_{ex}}{dt} = A_{ex} \cdot L \cdot \left(\bar{h}_{ex} \cdot \frac{\partial \bar{\rho}_{ex}}{\partial P_{ex}} - 1 \right) \cdot \frac{dP_{ex}}{dt} + \frac{1}{2} \cdot A_{ex} \cdot L \cdot \left(\bar{h}_{ex} \cdot \frac{\partial \bar{\rho}_{ex}}{\partial \bar{h}_{ex}} + \bar{\rho}_{ex} \right) \cdot \frac{dh_{h,o}}{dt} \quad (2.31)$$

Finally, replacing the previous values in the equation (2.27), we obtain:

$$\begin{aligned} &A_{ex} \cdot L \cdot \left(\bar{h}_{ex} \cdot \frac{\partial \bar{\rho}_{ex}}{\partial P_{ex}} - 1 \right) \cdot \frac{dP_{ex}}{dt} + \frac{1}{2} \cdot A_{ex} \cdot L \cdot \left(\bar{h}_{ex} \cdot \frac{\partial \bar{\rho}_{ex}}{\partial \bar{h}_{ex}} + \bar{\rho}_{ex} \right) \cdot \frac{dh_{h,o}}{dt} \\ &= -\dot{Q}_\ell - \dot{Q}_{L-\ell} + \dot{m}_{in,ex} \cdot h_{h,i} - \dot{m}_{o,ex} \cdot h_{h,o} \end{aligned} \quad (2.32)$$

2.8 Combination of equations

At this moment, we have the equations that govern the behavior of the evaporator, but to solve it, its necessary to arrange and make combination of all the above equations. To obtain a coherent system of equations, we solve for the mass flow $\dot{m}(\ell)$ from the equations (2.1) and (2.10) . Obtaining the equations (2.33) and (2.34), which are replaced in the equations (2.14) and (2.19),

to finally obtain the equations:

$$\dot{m}(\ell) = \dot{m}_4 - \frac{dm_\ell}{dt} \quad (2.33)$$

and:

$$\dot{m}(\ell) = \frac{dm_{L-\ell}}{dt} + \dot{m}_1 \quad (2.34)$$

Equating expressions (2.33) and (2.34), we obtain:

$$\dot{m}_4 - \frac{dm_\ell}{dt} = \frac{dm_{L-\ell}}{dt} + \dot{m}_1 \quad (2.35)$$

Replacing the equations (2.8) and (2.13), in the expression (2.35), we obtain the equation (2.36):

$$\begin{aligned} & \dot{m}_4 - \left[(\rho_v - \rho_l) \cdot A \cdot \ell \cdot \frac{d\bar{\gamma}}{dt} + (\bar{\gamma} \cdot \rho_v + (1 - \bar{\gamma}) \cdot \rho_l) \cdot A \cdot \frac{d\ell}{dt} \right. \\ & \left. + \left(\bar{\gamma} \cdot \frac{\partial \rho_v}{\partial P} + (1 - \bar{\gamma}) \cdot \frac{\partial \rho_l}{\partial P} \right) \cdot A \cdot \ell \cdot \frac{dP}{dt} \right] \\ = & A \cdot (L - \ell) \cdot \left(\frac{\partial \bar{\rho}_g}{\partial P} + \frac{1}{2} \cdot \frac{\partial \bar{\rho}_g}{\partial h_g} \cdot \frac{\partial h_v}{\partial P} \right) \cdot \frac{dP}{dt} + A \cdot (L - \ell) \cdot \frac{1}{2} \cdot \frac{\partial \bar{\rho}_g}{\partial h_g} \cdot \frac{dh_{out}}{dt} - \bar{\rho}_g \cdot A \cdot \frac{d\ell}{dt} + \dot{m}_1 \end{aligned} \quad (2.36)$$

This combined mass equation expresses the rate of change of the mass within the internal fluid-side heat exchanger with respect to time. Finally, this equation for the conservation of total mass can be expressed as the equation, where the term on the left side of the equality expresses the difference between the inlet and outlet mass flow of the heat exchanger (2.37):

$$\begin{aligned} \dot{m}_4 - \dot{m}_1 = & \left(A \cdot (L - \ell) \cdot \left(\frac{\partial \bar{\rho}_g}{\partial P} + \frac{1}{2} \cdot \frac{\partial \bar{\rho}_g}{\partial h_g} \cdot \frac{\partial h_v}{\partial P} \right) + \left(\bar{\gamma} \cdot \frac{\partial \rho_v}{\partial P} + (1 - \bar{\gamma}) \cdot \frac{\partial \rho_l}{\partial P} \right) \cdot A \cdot \ell \right) \cdot \frac{dP}{dt} \\ & + A \cdot (L - \ell) \cdot \frac{1}{2} \cdot \frac{\partial \bar{\rho}_g}{\partial h_g} \cdot \frac{dh_{out}}{dt} \\ & + (\rho_v - \rho_l) \cdot A \cdot \ell \cdot \frac{d\bar{\gamma}}{dt} + (\bar{\gamma} \cdot \rho_v + (1 - \bar{\gamma}) \cdot \rho_l - \bar{\rho}_g) \cdot A \cdot \frac{d\ell}{dt} \end{aligned} \quad (2.37)$$

In the same way, the coupling of the previous energy conservation equations must be carried out, starting with:

$$\frac{dU_\ell}{dt} = \dot{Q}_\ell + \dot{m}_4 \cdot h_4 - \dot{m}_\ell \cdot h_\ell \quad (2.38)$$

And:

$$\frac{dU_{L-\ell}}{dt} = \dot{Q}_{L-\ell} + \dot{m}_\ell \cdot h_\ell - \dot{m}_1 \cdot h_1 \quad (2.39)$$

Replacing equation (2.33) in (2.14), we obtain the equation (2.40):

$$\frac{dU_\ell}{dt} = \dot{Q}_\ell + \dot{m}_4 \cdot (h_4 - h_v) + \frac{dm_\ell}{dt} \cdot h_v \quad (2.40)$$

Replacing the variation of internal energy in the two phase region with respect to time, and the variation of mass in the two phase region, from the previous section, the following equality are obtained:

$$\begin{aligned} & (\rho_v \cdot h_v - \rho_\ell \cdot h_\ell) \cdot A \cdot \ell \cdot \frac{d\bar{\gamma}}{dt} + (\bar{\gamma} \cdot \rho_v h_v + (1 - \bar{\gamma}) \cdot \rho_\ell \cdot h_\ell - P) \cdot A \cdot \frac{d\ell}{dt} \\ & + \left(\bar{\gamma} \left(\frac{\partial \rho_v}{\partial P} \cdot h_v + \frac{\partial h_v}{\partial P} \cdot \rho_v \right) + (1 - \bar{\gamma}) \left(\frac{\partial \rho_\ell}{\partial P} \cdot h_\ell + \frac{\partial h_\ell}{\partial P} \cdot \rho_\ell \right) - 1 \right) \cdot A \cdot \ell \cdot \frac{dP}{dt} = \dot{Q}_\ell + \dot{m}_4 \cdot (h_4 - h_v) \\ & + \left((\rho_v - \rho_\ell) \cdot A \cdot \ell \cdot \frac{d\bar{\gamma}}{dt} + \left(\bar{\gamma} \cdot \frac{\partial \rho_v}{\partial P} + (1 - \bar{\gamma}) \frac{\partial \rho_\ell}{\partial P} \right) \cdot A \cdot \ell \cdot \frac{dP}{dt} + (\bar{\gamma} \cdot \rho_v + (1 - \bar{\gamma}) \cdot \rho_\ell) \cdot A \cdot \frac{d\ell}{dt} \right) \cdot h_v \end{aligned} \quad (2.41)$$

$$\begin{aligned} & (\rho_v \cdot h_v - \rho_\ell \cdot h_\ell) \cdot A \cdot \ell \cdot \frac{d\bar{\gamma}}{dt} + (\bar{\gamma} \cdot \rho_v h_v + (1 - \bar{\gamma}) \cdot \rho_\ell \cdot h_\ell - P) \cdot A \cdot \frac{d\ell}{dt} \\ & + \left(\bar{\gamma} \left(\frac{\partial \rho_v}{\partial P} \cdot h_v + \frac{\partial h_v}{\partial P} \cdot \rho_v \right) + (1 - \bar{\gamma}) \left(\frac{\partial \rho_\ell}{\partial P} \cdot h_\ell + \frac{\partial h_\ell}{\partial P} \cdot \rho_\ell \right) - 1 \right) \cdot A \cdot \ell \cdot \frac{dP}{dt} = \dot{Q}_\ell + \dot{m}_4 \cdot (h_4 - h_v) \\ & + (\rho_v \cdot h_v - \rho_\ell \cdot h_v) \cdot A \cdot \ell \cdot \frac{d\bar{\gamma}}{dt} + \left(\bar{\gamma} \cdot h_v \cdot \frac{\partial \rho_v}{\partial P} + (1 - \bar{\gamma}) \cdot h_v \frac{\partial \rho_\ell}{\partial P} \right) \cdot A \cdot \ell \cdot \frac{dP}{dt} \\ & + (\bar{\gamma} \cdot \rho_v \cdot h_v + (1 - \bar{\gamma}) \cdot \rho_\ell \cdot h_v) \cdot A \cdot \frac{d\ell}{dt} \end{aligned} \quad (2.42)$$

$$\begin{aligned} & (\rho_\ell \cdot (h_v - h_\ell)) \cdot A \cdot \ell \cdot \frac{d\bar{\gamma}}{dt} + ((1 - \bar{\gamma}) \cdot \rho_\ell \cdot (h_\ell - h_v) - P) \cdot A \cdot \frac{d\ell}{dt} \\ & + \left(\bar{\gamma} \cdot \frac{\partial h_v}{\partial P} \cdot \rho_v + (1 - \bar{\gamma}) \cdot \frac{\partial \rho_\ell}{\partial P} \cdot (h_\ell - h_v) + (1 - \bar{\gamma}) \frac{\partial h_\ell}{\partial P} \cdot \rho_\ell - 1 \right) \cdot A \cdot \ell \cdot \frac{dP}{dt} = \dot{Q}_\ell + \dot{m}_4 \cdot (h_4 - h_v) \end{aligned} \quad (2.43)$$

In a similar way to the situation presented above, equations (2.23) and (2.13) are obtained

as final result after mathematical arrangements the expression given in (2.45).

$$\begin{aligned}
& \left(\frac{\partial \bar{\rho}_g}{\partial P} \cdot \bar{h}_g + \frac{\partial \bar{\rho}_g}{\partial \bar{h}_g} \cdot \frac{1}{2} \cdot \frac{\partial h_v}{\partial P} \cdot \bar{h}_g + \bar{\rho}_g \cdot \frac{1}{2} \cdot \frac{\partial h_v}{\partial P} - 1 \right) \cdot A \cdot (L - \ell) \cdot \frac{dP}{dt} \\
& + \left(\frac{1}{2} \cdot \frac{\partial \bar{\rho}_g}{\partial \bar{h}_g} \cdot \bar{h}_g + \frac{1}{2} \cdot \bar{\rho}_g \right) \cdot A \cdot (L - \ell) \cdot \frac{dh_{out}}{dt} \\
& + (P - \bar{\rho}_g \cdot \bar{h}_g) \cdot A \cdot \frac{d\ell}{dt} = \dot{Q}_{L-\ell} + \dot{m}_1 \cdot (h_v - h_1) + h_v \cdot \left(\frac{\partial \bar{\rho}_g}{\partial P} + \frac{\partial \bar{\rho}_g}{\partial \bar{h}_g} \cdot \frac{1}{2} \cdot \frac{\partial h_v}{\partial P} \right) \cdot A \cdot (L - \ell) \frac{dP}{dt} \\
& + h_v \cdot A \cdot (L - \ell) \cdot \frac{1}{2} \frac{\partial \bar{\rho}_g}{\partial \bar{h}_g} \cdot \frac{dh_{out}}{dt} - h_v \cdot \bar{\rho}_g \cdot A \cdot \frac{d\ell}{dt}
\end{aligned} \tag{2.44}$$

$$\begin{aligned}
& \left(\frac{\partial \bar{\rho}_g}{\partial P} \cdot (\bar{h}_g - h_v) + \frac{\partial \bar{\rho}_g}{\partial \bar{h}_g} \cdot \frac{1}{2} \cdot \frac{\partial h_v}{\partial P} \cdot (\bar{h}_g - h_v) + \frac{1}{2} \cdot \bar{\rho}_g \cdot \frac{\partial h_v}{\partial P} - 1 \right) \cdot A \cdot (L - \ell) \cdot \frac{dP}{dt} \\
& + \left(\frac{1}{2} \cdot \frac{\partial \bar{\rho}_g}{\partial \bar{h}_g} \cdot (\bar{h}_g - h_v) + \frac{1}{2} \bar{\rho}_g \right) \cdot A \cdot (L - \ell) \cdot \frac{dh_{out}}{dt} + (P + \bar{\rho}_g \cdot (h_v - \bar{h}_g)) \cdot A \frac{d\ell}{dt} \\
& = \dot{Q}_{L-\ell} + \dot{m}_1 \cdot (h_v - h_1)
\end{aligned} \tag{2.45}$$

Combining the equations and considering that $\frac{d\gamma}{dt}$ is negligible [19], the following system of first order differential equations can be reached:

$$\begin{bmatrix} z_{11} & z_{12} & z_{13} & 0 & 0 \\ 0 & 0 & 0 & z_{24} & z_{25} \\ 0 & 0 & 0 & z_{34} & z_{35} \\ z_{41} & 0 & z_{43} & 0 & 0 \\ z_{51} & z_{52} & z_{53} & 0 & 0 \end{bmatrix} \cdot \begin{bmatrix} \dot{P} \\ \dot{h}_{out} \\ \dot{\ell} \\ \dot{P}_{ex} \\ \dot{h}_{h,o} \end{bmatrix} = \begin{bmatrix} f_1 \\ f_2 \\ f_3 \\ f_4 \\ f_5 \end{bmatrix} \tag{2.46}$$

With $\dot{P} = \frac{dP}{dt}$, $\dot{h}_{out} = \frac{dh_{out}}{dt}$, $\dot{\ell} = \frac{d\ell}{dt}$, $\dot{P}_{ex} = \frac{d\bar{P}_{ex}}{dt}$ and $\dot{h}_{h,o} = \frac{dh_{h,o}}{dt}$ and the components $z_{i,j}$, $1 \leq i \leq 5$, $1 \leq j \leq 5$ of the matrix and the components f_i , $1 \leq i \leq 5$ of right hand side vector detailed in Table 2.1. It is worth noting that:

- this system of differential equations is non-linear, each of the terms $z_{i,j}$ depending on some of the unknowns of the problem.
- it cannot be solved by traditional numerical algorithm if maintained in this form. Its

Array elements	Value
z_{11}	$A \cdot (L - \ell) \cdot \left(\frac{\partial \bar{\rho}_g}{\partial P} + \frac{1}{2} \cdot \frac{\partial \bar{\rho}_g}{\partial h_g} \cdot \frac{\partial h_v}{\partial P} \right) + \left(\bar{\gamma} \cdot \frac{\partial \rho_v}{\partial P} + (1 - \bar{\gamma}) \cdot \frac{\partial \rho_\ell}{\partial P} \right) \cdot A \cdot \ell$
z_{12}	$A \cdot (L - \ell) \cdot \frac{1}{2} \frac{\partial \bar{\rho}_g}{\partial h_g}$
z_{13}	$(\bar{\gamma} \cdot \rho_v + (1 - \bar{\gamma}) \cdot \rho_\ell - \bar{\rho}_g) \cdot A$
z_{24}	$A_e \cdot L \cdot \frac{\partial \bar{\rho}_{ex}}{\partial P_{ex}}$
z_{25}	$A_e \cdot L \cdot \frac{1}{2} \cdot \frac{\partial \bar{\rho}_{ex}}{\partial h_{ex}}$
z_{34}	$A_{ex} \cdot L \cdot \left(\bar{h}_{ex} \cdot \frac{\partial \bar{\rho}_{ex}}{\partial P_{ex}} - 1 \right)$
z_{35}	$\frac{1}{2} \cdot A_{ex} \cdot L \cdot \left(\bar{h}_{ex} \cdot \frac{\partial \bar{\rho}_{ex}}{\partial h_{ex}} + \bar{\rho}_{ex} \right)$
z_{41}	$\left(\bar{\gamma} \cdot \frac{\partial h_v}{\partial P} \cdot \rho_v + (1 - \bar{\gamma}) \cdot \frac{\partial \rho_\ell}{\partial P} \cdot (h_\ell - h_v) + (1 - \bar{\gamma}) \frac{\partial h_\ell}{\partial P} \cdot \rho_\ell - 1 \right) \cdot A \cdot \ell$
z_{43}	$\left((1 - \bar{\gamma}) \cdot \rho_\ell \cdot (h_\ell - h_v) - P \right) \cdot A$
z_{51}	$\left(\frac{\partial \bar{\rho}_g}{\partial P} \cdot (\bar{h}_g - h_v) + \frac{\partial \bar{\rho}_g}{\partial h_g} \cdot \frac{1}{2} \cdot \frac{\partial h_v}{\partial P} \cdot (\bar{h}_g - h_v) + \frac{1}{2} \cdot \bar{\rho}_g \cdot \frac{\partial h_v}{\partial P} - 1 \right) \cdot A \cdot (L - \ell)$
z_{52}	$\left(\frac{1}{2} \cdot \frac{\partial \bar{\rho}_g}{\partial h_g} \cdot (\bar{h}_g - h_v) + \frac{1}{2} \bar{\rho}_g \right) \cdot A \cdot (L - \ell)$
z_{53}	$(P + \bar{\rho}_g \cdot (h_v - \bar{h}_g)) \cdot A$
f_1	$\dot{m}_4 - \dot{m}_1$
f_2	$\dot{m}_{in,ex} - \dot{m}_{o,ex}$
f_3	$-\dot{Q}_\ell - \dot{Q}_{L-\ell} + \dot{m}_{in,ex} \cdot h_{h,i} - \dot{m}_{o,ex} \cdot h_{h,o}$
f_4	$\dot{Q}_\ell + \dot{m}_4 \cdot (h_4 - h_v)$
f_5	$\dot{Q}_{L-\ell} + \dot{m}_1 \cdot (h_v - h_1)$

Table 2.1: Array elements of differential equations

expression will be modified for so.

Chapter III

Solution algorithm development

To solve the problem, a Python¹ code has been developed, which allows the aforementioned calculations to be carried out, using specific libraries dedicated to numerical computations, i.e. numpy² and scipy³. The solving process can be described by the flow chart shown in Figure 3.1.

3.1 Incorporation of thermodynamic properties

To compute the fluids thermodynamic properties, the CoolProp library⁴ is used, which allows the use of various common fluids such as R22, R414, CO2, among others. For the calculation of the derivatives of the state variables, CoolProp library in version 6.3 was used. This value is verified by calculating the properties using the finite difference method.

3.2 Variable initialization

During program initialization, the user has to enter the working fluid, in addition to the initial conditions. Given that for the mobile contour model, the lengths corresponding to each phase

¹<https://www.python.org/>.

²<https://numpy.org/>.

³<https://scipy.org/>.

⁴<http://www.coolprop.org/>.

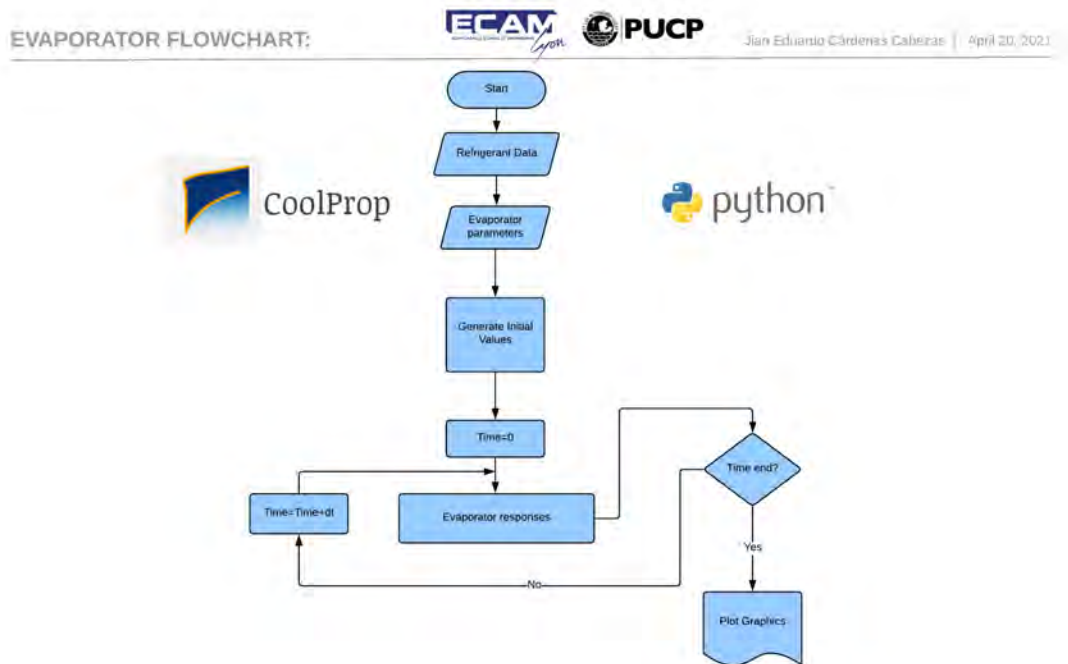


Figure 3.1: Flow Chart of the complete solving process.

of the fluid are required in heat exchangers (wet steam or superheated steam), it is necessary to previously determine these values, it should be added that these values are not experimental, so the steady state analysis should be applied.

In order to obtain these required parameters, it is necessary to perform iterative calculations, in which a convergence is reached for the length and temperature corresponding to the two phase region. The flow diagram in the figure 3.2 shows the logic developed to obtain these parameters.

3.3 Solving of differential equation

In order to be treated by any numerical algorithm, a system of differential equations has to be written as the standard form:

$$\frac{dy}{dt}(t) = F(t, \mathbf{y}(t)) \quad (3.1)$$

with $\mathbf{y}(t) = (y_1(t) \ y_2(t) \ \dots \ y_n(t))^T$ the vector containing the n unknowns $y_i, 1 \leq i \leq n$ of the problem, and $F : \mathbb{R}^n \mapsto \mathbb{R}^n$ which can be almost any kind of function. When compared with

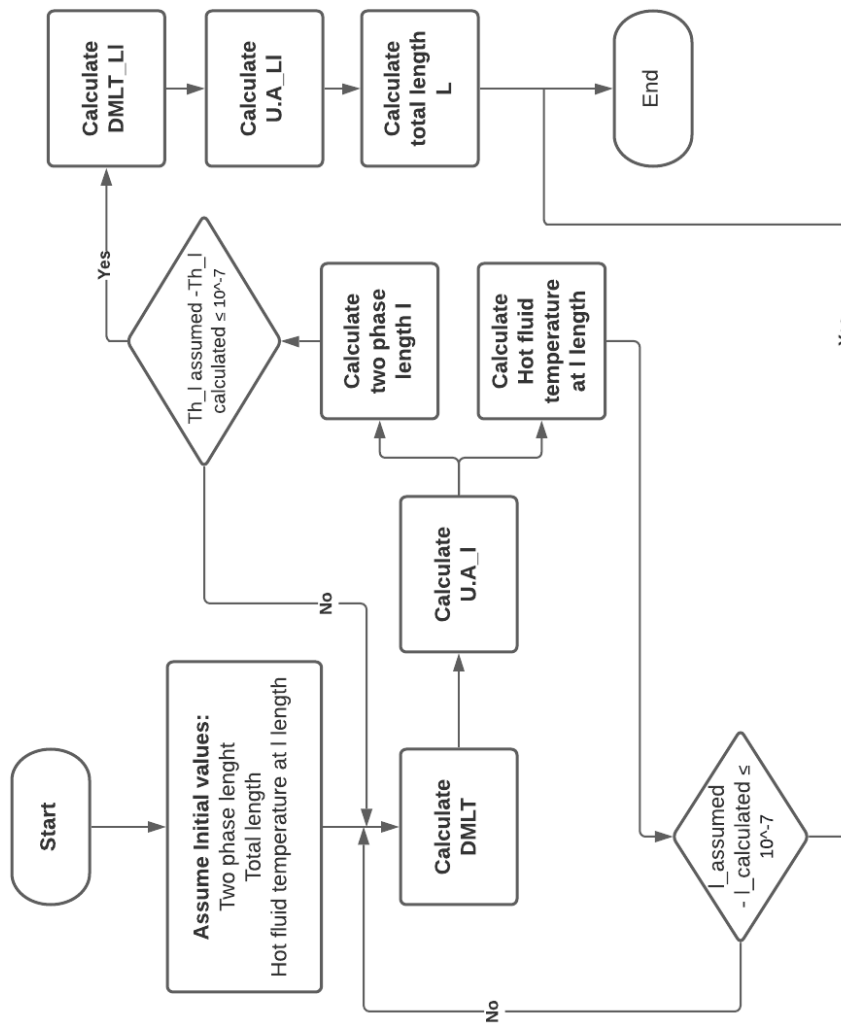


Figure 3.2: Steady state flow chart.

equation (2.46), it is clear that the latter needs to be involve in a diagonalization process in order to meet with the required form of equation (3.1).

Accordingly, in order to solve the matrix of differential equations, the ODEINT library from scipy has been used, which requires the equations in the form of a column matrix consistent with equation (3.1). To be able to use it in the code, its diagonalization has been carried out, obtaining

the matrix of equation (3.2):

$$\begin{bmatrix} 1 & 0 & 0 & 0 & 0 \\ 0 & 1 & 0 & 0 & 0 \\ 0 & 0 & 1 & 0 & 0 \\ 0 & 0 & 0 & 1 & 0 \\ 0 & 0 & 0 & 0 & 1 \end{bmatrix} \cdot \begin{bmatrix} \dot{P} \\ \dot{h}_{out} \\ \dot{\ell} \\ \dot{P}_{ex} \\ \dot{h}_{h,o} \end{bmatrix} = \begin{bmatrix} \dot{P} \\ \dot{h}_{out} \\ \dot{\ell} \\ \dot{P}_{ex} \\ \dot{h}_{h,o} \end{bmatrix} = \begin{bmatrix} a + b - c \\ d + e + f \\ g + h + i \\ \frac{f_2 \cdot z_{35}}{z_{24} \cdot z_{35} - z_{25} \cdot z_{34}} - \frac{f_3 \cdot z_{25}}{z_{24} \cdot z_{35} - z_{25} \cdot z_{34}} \\ -\frac{f_2 \cdot z_{34}}{z_{24} \cdot z_{35} - z_{25} \cdot z_{34}} + \frac{f_3 \cdot z_{24}}{z_{24} \cdot z_{35} - z_{25} \cdot z_{34}} \end{bmatrix} \quad (3.2)$$

With terms a to i detailed in Table 3.1 and $z_{i,j}$ and f_j in Table 2.1 of page 17.

Array elements	Value
a	$\frac{f_1 \cdot z_{43} \cdot z_{52}}{z_{11} \cdot z_{43} \cdot z_{52} + z_{12} \cdot z_{41} \cdot z_{53} - z_{12} \cdot z_{43} \cdot z_{51} - z_{13} \cdot z_{41} \cdot z_{52}}$
b	$\frac{f_4 \cdot (z_{12} \cdot z_{53} - z_{13} \cdot z_{52})}{z_{11} \cdot z_{43} \cdot z_{52} + z_{12} \cdot z_{41} \cdot z_{53} - z_{12} \cdot z_{43} \cdot z_{51} - z_{13} \cdot z_{41} \cdot z_{52}}$
c	$\frac{f_5 \cdot z_{12} \cdot z_{43}}{z_{11} \cdot z_{43} \cdot z_{52} + z_{12} \cdot z_{41} \cdot z_{53} - z_{12} \cdot z_{43} \cdot z_{51} - z_{13} \cdot z_{41} \cdot z_{52}}$
d	$\frac{f_1 \cdot (z_{41} \cdot z_{53} - z_{43} \cdot z_{51})}{z_{11} \cdot z_{43} \cdot z_{52} + z_{12} \cdot z_{41} \cdot z_{53} - z_{12} \cdot z_{43} \cdot z_{51} - z_{13} \cdot z_{41} \cdot z_{52}}$
e	$\frac{f_4 \cdot (-z_{11} \cdot z_{53} + z_{13} \cdot z_{51})}{z_{11} \cdot z_{43} \cdot z_{52} + z_{12} \cdot z_{41} \cdot z_{53} - z_{12} \cdot z_{43} \cdot z_{51} - z_{13} \cdot z_{41} \cdot z_{52}}$
f	$\frac{f_5 \cdot (z_{11} \cdot z_{43} - z_{13} \cdot z_{41})}{z_{11} \cdot z_{43} \cdot z_{52} + z_{12} \cdot z_{41} \cdot z_{53} - z_{12} \cdot z_{43} \cdot z_{51} - z_{13} \cdot z_{41} \cdot z_{52}}$
g	$-\frac{f_1 \cdot z_{41} \cdot z_{52}}{z_{11} \cdot z_{43} \cdot z_{52} + z_{12} \cdot z_{41} \cdot z_{53} - z_{12} \cdot z_{43} \cdot z_{51} - z_{13} \cdot z_{41} \cdot z_{52}}$
h	$\frac{f_4 \cdot (z_{11} \cdot z_{52} - z_{12} \cdot z_{51})}{z_{11} \cdot z_{43} \cdot z_{52} + z_{12} \cdot z_{41} \cdot z_{53} - z_{12} \cdot z_{43} \cdot z_{51} - z_{13} \cdot z_{41} \cdot z_{52}}$
i	$\frac{f_5 \cdot z_{12} \cdot z_{41}}{z_{11} \cdot z_{43} \cdot z_{52} + z_{12} \cdot z_{41} \cdot z_{53} - z_{12} \cdot z_{43} \cdot z_{51} - z_{13} \cdot z_{41} \cdot z_{52}}$

Table 3.1: Array elements of matrix column in equation (3.2).

Chapter IV

Numerical treatment of the model

4.1 Experimental correlations

To test the model, a numerical simulation of an evaporator operating with CO_2 has been carried out. The input data for the steady-state calculation were those shown in Table 4.1. With this

Variable	Value
Cold fluid	CO_2
Hot fluid	H_2O
Inside diameter	0.01 m
External diameter	0.015 m
Saturation Temperature	268.15 K
Cold fluid mass flow	0.02 kg/s
Cold fluid exit temperature	278.15 K
Cold fluid inlet enthalpy	265.274 kJ/kg
Hot fluid mass flow	0.025 kg/s
Hot fluid pressure	300000 Pa
Hot fluid inlet temperature	313.15 K

Table 4.1: Input data for steady state calculation

input data, it is possible to determine all the remaining geometric features. However, one of the main limitations is obtaining the convective coefficient in the two-phase region. From the literature consulted, most of the analytical expressions provide underestimated values when compared to experimental ones. In 2006, Cheng et al. [7], carried out an analysis with more than 2000 data and obtained a correlation that has a very good precision with respect to the

experimentation. However, this correlation requires some further experimental values in order to be used. In the present work, a sensitivity analysis of the value of the convective coefficient was carried out, in the valid range of the correlation found in [7].

This correlation is valid as long as the following criteria are satisfied:

- Saturation temperature: $-28^{\circ}\text{C} \leq T_{sat} \leq 25^{\circ}\text{C}$.
- Heat flux: $5 \frac{\text{kW}}{\text{m}^2} \leq q \leq 32 \frac{\text{kW}}{\text{m}^2}$.
- Mass velocity: $170 \frac{\text{kg}}{\text{m}^2 \cdot \text{s}} \leq G \leq 570 \frac{\text{kg}}{\text{m}^2 \cdot \text{s}}$.
- Hydraulic diameter: $0.8\text{mm} \leq D \leq 10\text{mm}$.

The values considered for the numerical treatment satisfy the criteria previously stated.

4.2 Determination of length ℓ and total length of the evaporator

As stated above, the value of the evaporation length ℓ and of the total length L of the evaporator are functions of the two phase convective coefficient. With these input data, the main unknown being the length of the heat exchanger, the LMTD method [5] can be used to determine the heat exchange area and thereby determine the desired lengths.

The evaporator is divided into two parts, two-phase and superheated, in which to apply the LMTD method, it is necessary to know the temperature of the hot fluid, $T_{h\ell}$, at which the phase change occurs in the fluid cold. In order to determine this temperature, the heat exchange in a fluid differential is analyzed, as shown in the figure Figure 4.1

In the present analysis, the spatial dependence of the temperature of the hot fluid is taken into account.

$$\dot{m} \cdot c_p \cdot (T_{h,z} - T_{h,z+dz}) = U \cdot A \cdot \frac{dz}{L_{Total}} \cdot (T_{h,z} - T_{ref}) \quad (4.1)$$

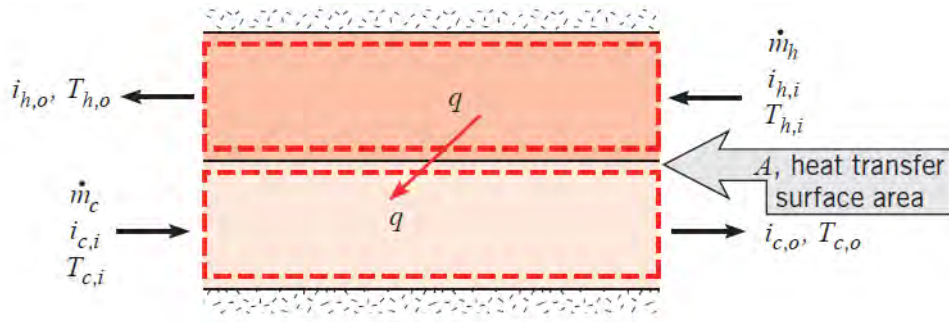


Figure 4.1: Differential of heat transfer analysis.

$$\frac{-dT}{T_{h,z} - T_{ref}} = \frac{U \cdot A \cdot dz}{L \cdot \dot{m} \cdot c_p} \quad (4.2)$$

$$\int_{T_{h,\ell}}^{T_{h,o}} \frac{-dT}{T_{h,z} - T_{ref}} = \int_{L-\ell}^L \frac{U \cdot A \cdot dz}{L \cdot \dot{m} \cdot c_p} \quad (4.3)$$

$$T_{h,\ell} = T_{ref} + \frac{(T_{h,o} - T_{ref})}{\exp \frac{-U \cdot A \cdot \ell}{L \cdot \dot{m} \cdot c_p}} \quad (4.4)$$

Obtaining in this way an exponential distribution of the variation of the temperature of the hot fluid. The Figure 4.2, shows a diagram of the temperature variation for each fluid inside the heat exchanger.

By obtaining this temperature value and performing iterations, it is possible to determine the value of the length of each phase within the evaporator using the LMTD method.

4.2.1 Calculation example

To show more clearly how to carry out the procedure stated above, an example of calculation was carried out.

In order to use the equation 4.4, the outlet temperature of the hot fluid must be determined. In order to determine this temperature, it is assumed that the heat exchanger is adiabatic, in which the heat exchange only occurs between the working fluids, then the heat transferred by

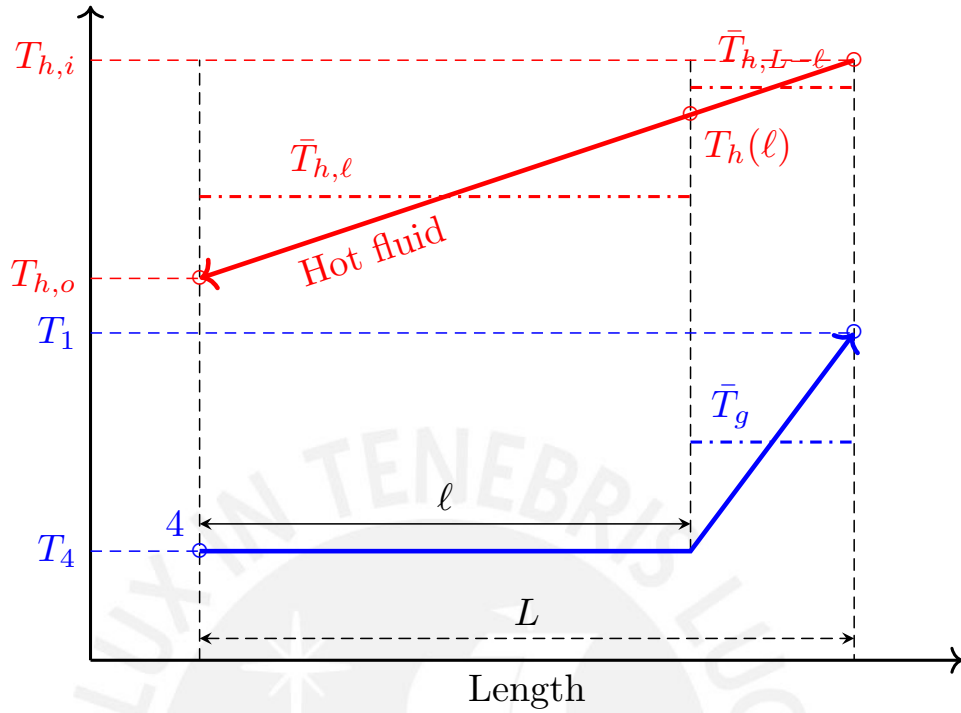


Figure 4.2: Temperature variation in the evaporator

the hot fluid is the same that reaches the cold fluid, such as shown in the equation 4.5:

$$\dot{Q} = \dot{m}_{CO_2} \cdot (h_{o,CO_2} - h_{i,CO_2}) = \dot{m}_{H_2O} \cdot (h_{i,H_2O} - h_{o,H_2O}) \quad (4.5)$$

From where, clearing the value of the enthalpy of the hot fluid, we have:

$$\begin{aligned} h_{o,H_2O} &= h_{i,H_2O} - \frac{\dot{m}_{CO_2} \cdot (h_{o,CO_2} - h_{i,CO_2})}{\dot{m}_{H_2O}} \\ &= 170.183 - \frac{0.02 \cdot (448.46 - 265.274)}{0.025} \\ &= 23.634 \frac{kJ}{kg} \end{aligned} \quad (4.6)$$

Since the outlet pressure and enthalpy for the hot fluid are known, the value of the outlet temperature can be determined, which has a value of 4.91°C.

In order to determine the LMTD value in the two phase region, the equation 4.7 is used [5]:

$$LMTD_{\ell} = \frac{T_{h,\ell} - T_{o,H_2O}}{\log\left(\frac{T_{h,\ell} - T_{ref}}{T_{o,H_2O} - T_{ref}}\right)} \quad (4.7)$$

However, in this expression the value of the temperature $T_{h,\ell}$ is unknown, and in order to calculate it it is required to know the value of the lengths ℓ , L and the heat transfer coefficient global. Therefore, in order to determine these values, an iterative process must be carried out. It should be noted that to calculate the global heat transfer coefficient, U , the value of the convective coefficient of carbon dioxide will be varied between its minimum and maximum value ($8000 - 12000 \text{ W/m}^2 \cdot \text{K}$) to see its influence in determining the desired lengths.

In the present calculation example, the following initial values were used:

- $\ell = 5m$
- $T_{h,\ell} = 22.45^{\circ}\text{C}$
- $L = 6m$

$$\begin{aligned} Q_{\ell} &= m_{i,CO_2} \cdot (h_g - h_{i,CO_2}) \\ &= 0.02 \cdot (433.383 - 265.274) \\ &= 3.36 \text{ kW} \end{aligned} \quad (4.8)$$

$$\begin{aligned} LMTD_{prev} &= \frac{22.45 - 4.913}{\ln\left(\frac{22.45+5}{4.913+5}\right)} \\ &= 17.22^{\circ}\text{C} \end{aligned} \quad (4.9)$$

$$\begin{aligned} U \cdot A_{\ell} &= \frac{Q_{\ell}}{LMTD_{\ell}} \\ &= \frac{3.36}{17.22} = 0.195 \frac{\text{kW}}{^{\circ}\text{C}} \end{aligned} \quad (4.10)$$

$$T_{h,\ell} = -5 + \frac{4.91 - (-5)}{\exp \frac{-195.5}{6 \cdot 0.025 \cdot 4173.9}} \quad (4.11)$$

$$= 42.03 \text{ } ^\circ\text{C}$$

From these results, in order to determine the lengths, the convective coefficients must be determined. In the superheated steam region and for the external fluid, the Gnielinski correlation is used, for gases and liquids, respectively. For the biphasic region, a sensitivity analysis is performed according to the range of values found in [7].

Then, the calculation of the convective coefficient for superheated steam is carried out, using the expressions 4.12, 4.13 and 4.14.

$$Re_{SH} = \frac{4 \cdot \dot{m}}{\pi \cdot d \cdot \mu} \quad (4.12)$$

$$Nu_{SH} = 0.0214 \cdot (Re^{0.8} - 100) \cdot Pr^{0.4} \quad (4.13)$$

$$\alpha_{SH} = \frac{Nu \cdot k}{d} \quad (4.14)$$

For the hot fluid, the Gnielinski expression is used for liquids using the hydraulic diameter for its calculation.

$$Re_{ext} = \frac{4 \cdot \dot{m}}{\pi \cdot d_h \cdot \mu} \quad (4.15)$$

$$Nu_{ext} = 0.012 \cdot (Re_{ext}^{0.87} - 280) \cdot Pr^{0.4} \quad (4.16)$$

$$\alpha_{ext} = \frac{Nu \cdot k}{d_h} \quad (4.17)$$

From this, it is observed that the assumed value of $T_{h,\ell}$ is very different from the calculated value, so more iterations are required to obtain the correct value. In this example, to reach the error of 10^{-6} , 39 iterations are required having as final values $T_{h,\ell} = 33.91^\circ\text{C}$, $\ell = 6.41\text{ m}$ and $L = 7.12\text{ m}$.



Chapter V

Model exploitation

With these initial values obtained, and through the variation of the inlet and outlet mass flow rates to and from the evaporator, it is possible to test the model previously presented. For the present analysis, a time step increase of evaporator outlet mass flow rate has been simulated, was made for the evaporator outlet flow and by means of a first order equation it is produced that at the entrance of the evaporator a variation in the shape of the curve is obtained until the steady state is reached again.

The equation 5.1 governs the behavior of the input mass flow.

$$\tau \cdot \frac{d\dot{m}_{4(t)}}{dt} + \dot{m}_{4(t)} = \dot{m}_{1(t-d)} \quad (5.1)$$

To be able to be coupled together with the system of equations in figure ?? of chapter 2, the variation of the input mass must be solved with respect to time, as shown in the equation 5.2.

$$\frac{d\dot{m}_{4(t)}}{dt} = \frac{\dot{m}_{1(t-d)} - \dot{m}_{4(t)}}{\tau} \quad (5.2)$$

In order to solve the system of differential equations, the Python ODEINT library was used, which allows solving systems of rigid differential equations.

The result of the different variables studied against a step-type variation is given by the figures 5.3 , 5.4 and 5.5.

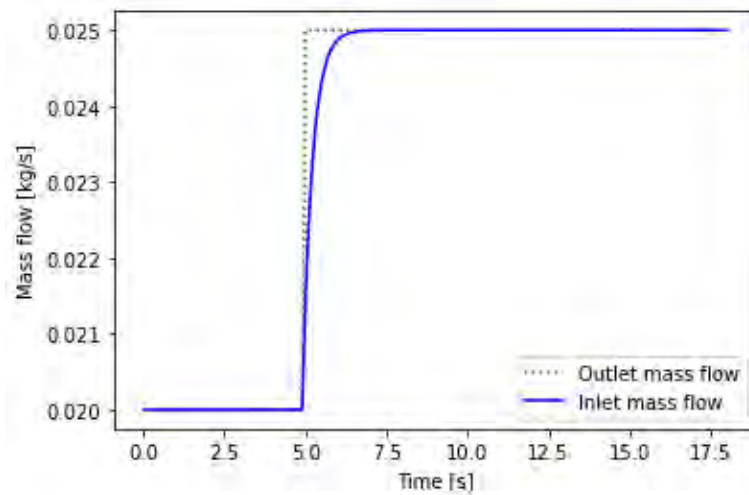


Figure 5.1: Mass flow vs time.

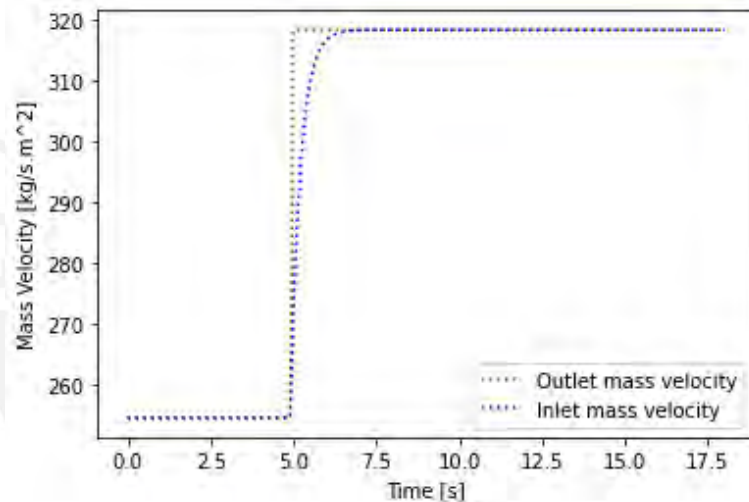


Figure 5.2: Mass velocity vs time.

Performing the same analysis but this time using the value of the convective coefficient as $8000 \frac{W}{m^2 \cdot K}$, the figures 5.6, 5.7 and 5.8 are obtained.

The Table 5.1 shows the variation of the results obtained when the convective coefficient is varied from 8000 to $12000 \frac{W}{m^2 \cdot K}$:

From the results obtained, it is observed that the greatest variation is 3 %, with which, we can say that despite not having a precise value of the convective coefficient in the biphasic region, it will not affect the determination of the others. parameters.

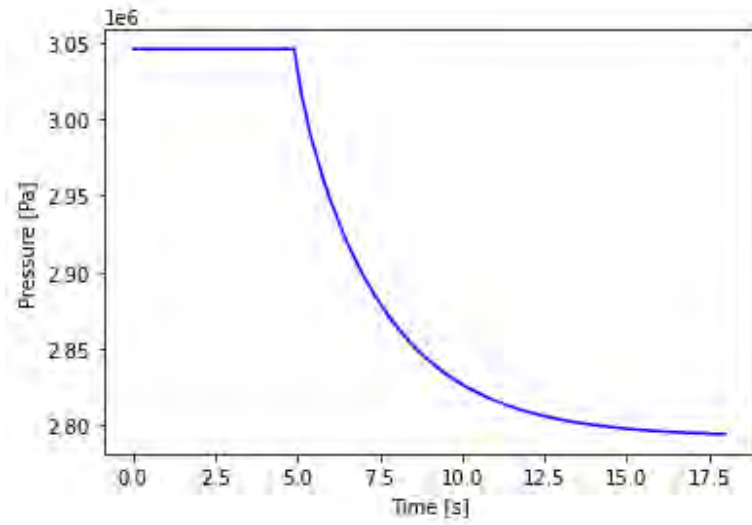


Figure 5.3: Carbon dioxide pressure vs time.

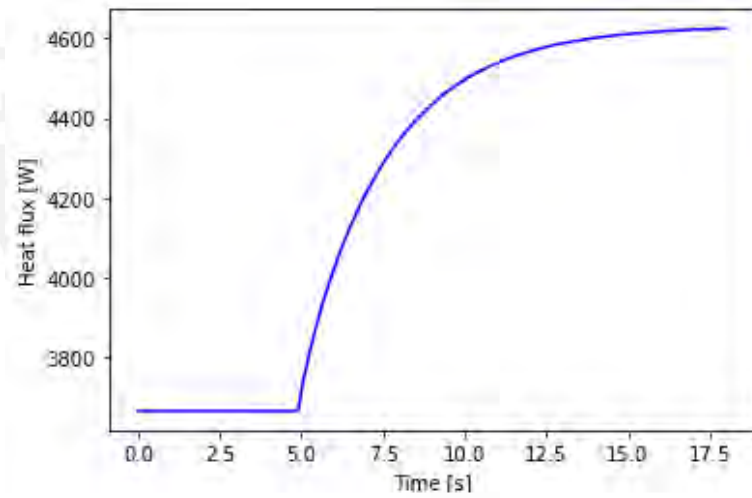


Figure 5.4: Total heat flux vs time.

Variable	$\alpha_{Tp} = 8000 \frac{W}{m^2 \cdot K}$	$\alpha_{Tp} = 12000 \frac{W}{m^2 \cdot K}$	Error(%)
Total Heat Flux	4625.31 W	4625.33 W	4.32×10^{-4}
Outlet CO_2 temperature	276.314 K	276.278 K	0.013
Two phase length	6.50305 m	6.30466 m	3.05
Total Length	7.324 m	7.124 m	2.73

Table 5.1: Error due to the variation of the convective coefficient in the biphasic region

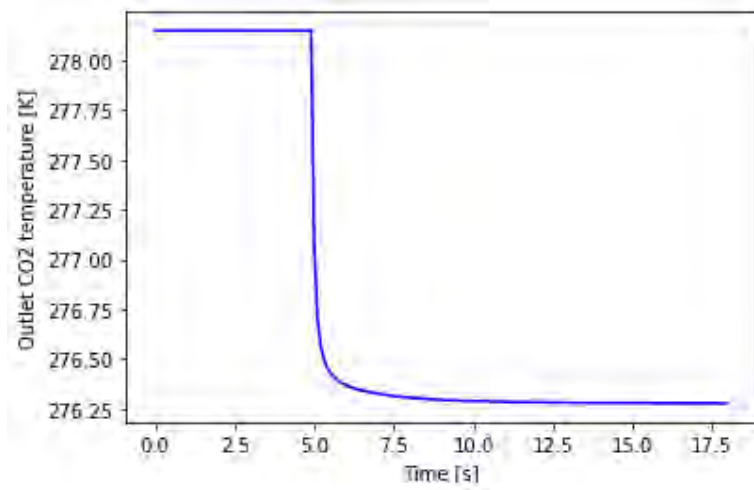


Figure 5.5: Outlet temperature vs time.

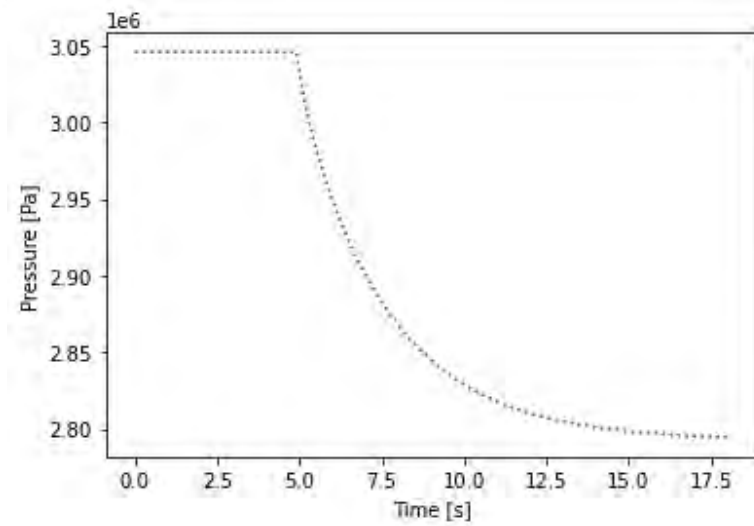


Figure 5.6: Carbon dioxide pressure vs time.

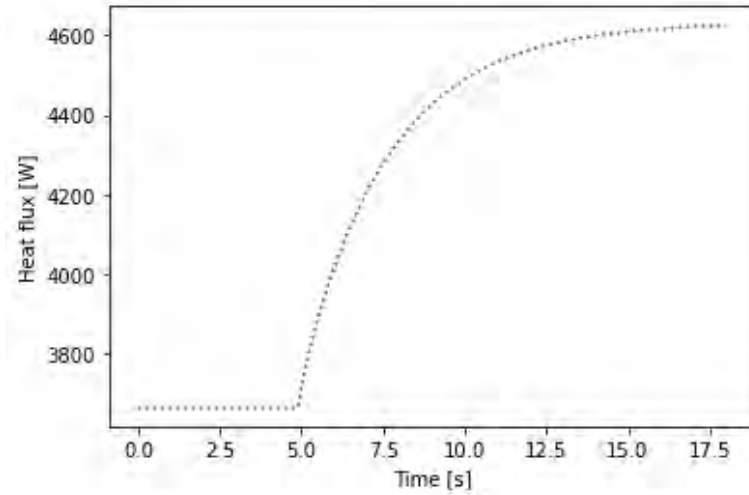


Figure 5.7: Total heat flux vs time.

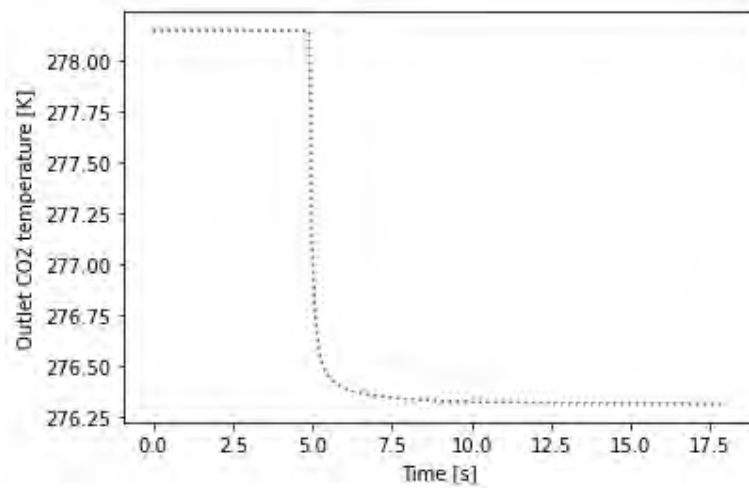


Figure 5.8: Outlet temperature vs time.

Chapter VI

Conclusion and perspectives

With the development of this thesis work, there is a better understanding of the physics involved in biphasic processes, in which physics is involved in the determination of the variables and not just a mathematical equation, and given the least amount of equations to be solved, the system can be adapted in the future to a control system.

An error in the calculation of the convective coefficient for the CO_2 does not translate into a big error in the determination of the most important parameters such as superheating (error $\approx 3\%$). This is reasonable, since the value of the convective coefficient in the biphasic region is much larger than the convective coefficient for the internal fluid, thus, the thermal resistance belonging to the convective coefficient of CO_2 is very low and does not affect the heat transfer [7], [1].

This thesis work presents many aspects to continue exploring. Some of the most salient ones will be listed below, including improvements in model validation, controller design, and modeling of more complex systems.

Regarding the validation of the model, in this thesis the validation of the model was carried out using numerical data, in which a variation is induced in the mass flow out of the evaporator (which in reality can be done by varying the speed compressor) and it is observed that after a certain time all the variables reach the steady state, however, in order to carry out a correct validation of the model, an experimentation must be carried out in a real refrigeration system.

The present thesis work forms an essential part in the development of a controller. This model is not really complete until it can actually be implemented in a controller and verified through experimentation.

The work developed only takes into account a component of the most basic refrigeration system, therefore, in future works, the complete model of the most basic refrigeration system (compressor, condenser, expansion valve and evaporator) can be developed and later develop the most complex system models, in which other components or arrangements are available, such as cascade refrigeration systems.



Bibliography

- [1] A. Aramburú Pardo Figueroa. Estudio de un sistema de refrigeración por compresión de vapor aplicado a la industria agroalimentaria. 2017.
- [2] P. Artuso, G. Tosato, A. Rossetti, S. Marinetti, A. Hafner, K. Banasiak, and S. Minetto. Dynamic modelling and validation of an air-to-water reversible r744 heat pump for high energy demand buildings. *Energies*, 14(24):8238, 2021.
- [3] A. M. Bahman, D. Ziviani, and E. A. Groll. A generalized moving-boundary algorithm to predict the heat transfer rate of transcritical co2 gas coolers. *International Journal of Refrigeration*, 118:491–503, 2020.
- [4] Y. Cengel and J. Cimbala. *Ebook: Fluid mechanics fundamentals and applications (si units)*. McGraw Hill, 2013.
- [5] Y. A. Cengel and A. J. Ghajar. Heat and mass transfer: fundamentals & applications. (*No Title*), 2011.
- [6] C. Changenet, J. Charvet, D. Gehin, F. Sicard, and B. Charmel. Study on predictive functional control of an expansion valve for controlling the evaporator superheat. *Proceedings of the Institution of Mechanical Engineers, Part I: Journal of Systems and Control Engineering*, 222(6):571–582, 2008.
- [7] L. Cheng, G. Ribatski, L. Wojtan, and J. R. Thome. New flow boiling heat transfer model and flow pattern map for carbon dioxide evaporating inside horizontal tubes. *International journal of heat and mass transfer*, 49(21-22):4082–4094, 2006.

- [8] J. Chi and D. Didion. A simulation model of the transient performance of a heat pump. *International Journal of refrigeration*, 5(3):176–184, 1982.
- [9] H. Fallahsohi, C. Changenet, S. Placé, G. Duhot, C. Ligeret, and X. Lin-Shi. Energy savings with advanced control of reciprocating liquid chillers. In *23rd International Conference on Efficiency, Cost, Optimization, Simulation (ECOS) and Environmental Impact*, volume 3, page 263, Lausanne, Switzerland, June 2010.
- [10] C. Gantz. *Refrigeration – A history*. McFarland & Compagny, 2015.
- [11] J. M. Jensen and H. Tummescheit. Moving boundary models for dynamic simulations of two-phase flows. In *Proc. of the 2nd Int. Modelica Conference*, volume 3. Oberpfaffenhofen Germany, 2002.
- [12] Q. Jin, J. T. Wen, and S. Narayanan. Moving boundary model for dynamic control of multi-evaporator cooling systems facing variable heat loads. *International Journal of Refrigeration*, 120:481–492, 2020.
- [13] B. Li. *Dynamic modeling, simulation, and control of transportation HVAC systems*. PhD thesis, University of Illinois at Urbana-Champaign, 2013.
- [14] W. Li. Simplified modeling analysis of mass flow characteristics in electronic expansion valve. *Applied Thermal Engineering*, 53(1):8–12, 2013.
- [15] J. MacArthur and E. Grald. Prediction of cyclic heat pump performance with a fully distributed model and a comparison with experimental data. *ASHRAE Trans.:(United States)*, 93(CONF-870620-), 1987.
- [16] J. W. MacArthur and E. W. Grald. Unsteady compressible two-phase flow model for predicting cyclic heat pump performance and a comparison with experimental data. *International Journal of refrigeration*, 12(1):29–41, 1989.
- [17] A. Magnus and H. Jerregard. *Modeling and control of vapor compression refrigeration systems*. PhD thesis, Linkoping institute of technology, 2008.

- [18] H. Qiao, C. R. Laughman, V. Aute, and R. Radermacher. An advanced switching moving boundary heat exchanger model with pressure drop. *International journal of refrigeration*, 65:154–171, 2016.
- [19] B. P. Rasmussen. Dynamic modeling for vapor compression systems—part i: Literature review. *HVAC&R Research*, 18(5):934–955, 2012.
- [20] J. Rees. *Refrigeration Nation*. The Johns Hopkins University Press, 2013.
- [21] O. Yildiz, M. Yilmaz, and A. Celik. Reduction of energy consumption and co2 emissions of hvac system in airport terminal buildings. *Building and Environment*, 208:108632, 2022.



Annex

1) Verification of the influence of the convective coefficient

As stated in Chapter I, the value chosen for the convective coefficient in the two phase region is very large compared to the convective coefficient of the hot fluid. This means that it is practically not a parameter that will modify the results since the thermal resistance involved with this variable is very low. To demonstrate this, the analytical calculation of the total thermal resistance in the two phase region and the value of the convection resistance of the cold fluid was carried out. It should be noted again that in the calculations, the value of the resistance corresponding to the wall of the internal pipe of the heat exchanger has been directly neglected.

The value of the thermal resistance by convection is given by the following expression:

$$R_{sat} = \frac{1}{h_{sat} \cdot A}$$

$$R_{sat} = \frac{1}{8000 \cdot 0.2238} = 5.585 \times 10^{-4}$$

Similarly, the calculation of the resistance on the outer fluid side can be calculated by the following expression:

$$R_{ext} = \frac{1}{h_{ext} \cdot A}$$

$$R_{ext} = \frac{1}{643.18 \cdot 0.2238} = 6.94 \times 10^{-3}$$

From the figure 0.1, it is observed that the total resistance of the system in the phase change region is described by the sum of the resistances corresponding to convection in the internal and external fluid, such as It is shown by the following equation.

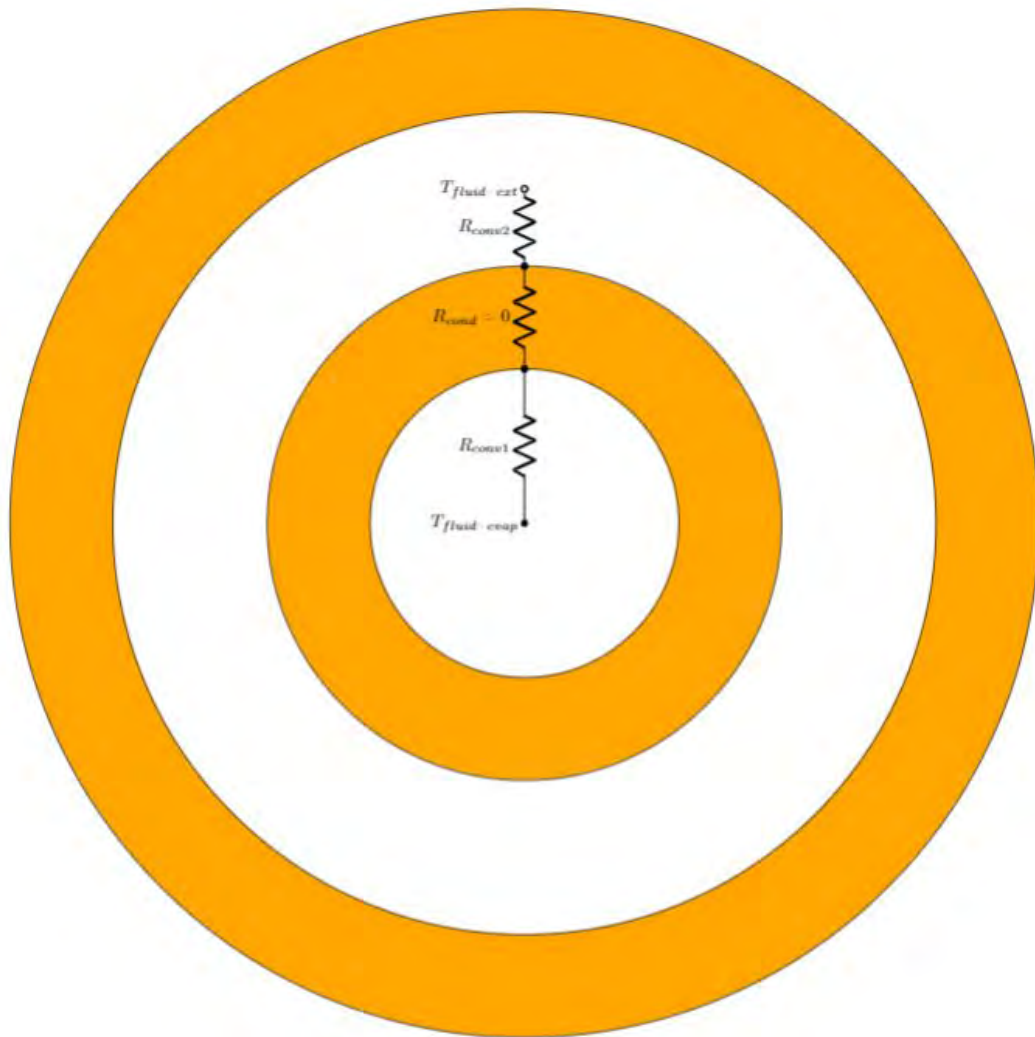


Figure 0.1: Resistances in the two phase region

$$R_{total} = R_{sat} + R_{ext}$$

$$R_{total} = 5.585 \times 10^{-4} + 6.94 \times 10^{-3} = 7.641 \times 10^{-3}$$

It is observed that the value of the resistance in the two phase region is 7 % of the total value of the resistance and if we increase the value of the two phase convective coefficient to 12000, it is obtained that it represents 5 %.

2) Void fraction calculation

In the present model used, it was considered that the void fraction does not vary with respect to time. In order to determine the average value in the evaporator, the Zivi model can be used, which is described by the following equations:

$$S = \left(\frac{\rho_f}{\rho_g} \right)^{\frac{1}{3}}$$

$$\bar{\gamma} = \frac{1}{\beta} + \frac{1}{x_2 - x_1} \cdot \left[\frac{\alpha}{\beta} \ln \left(\frac{\beta \cdot x_1 + \alpha}{\beta \cdot x_2 + \alpha} \right) \right]$$

where $\beta = 1 - \alpha$ and $\alpha = \left(\frac{\rho_g}{\rho_f} \right) \cdot S$. Replacing the values in the equations, we have that the value of the average vacuum fraction is 0.959.

3) Compressibility calculation

In order to determine if the fluid is compressible or not, the Mach number is calculated.

$$Ma = \frac{u}{c}$$

Where u is the velocity of the fluid and c is the speed of sound at the mean temperature.

In the example of calculation, the mass flow was fixed as 0.02 kg/s and the inner diameter of the pipe was 0.01 m. With this values the velocity inside the pipe is 0.49 m/s. For determine the

speed of sound, the temperature of evaporation was used in the CoolProp software. The mean speed of sound in the two phase region is 398.4 m/s.

Finally, the Mach number is 0.0012.

